Local thermal analysis using an optical fiber temperature sensor in a flow boiling heat transfer

Donghwi Lee [a,c*], Hyeon Taek Nam [c], and Seungro Lee [b,c*]
[a] *Department of Mechanical System Engineering, Jeonbuk National University, Korea*
[b] *Department of Mechanical Engineering, Jeonbuk National University, Korea*
[c] *Graduate School of Mechanical-Aerospace-Electric Convergence Engineering, Jeonbuk National University, Korea*
*Corresponding authors: dlee462@jbnu.ac.kr (D. Lee), seungrol@jbnu.ac.kr (S. Lee)

***Keywords : Optical fiber temperature sensor, Flow boiling heat transfer, Local thermal analysis**

1. Introduction

A flow boiling heat transfer is a crucial candidate for solving the rapidly increased demand for cooling technology owing to its high thermal efficiency [1-3]. In the boiling process, the phase change (from fluid to vapor) occurs with the absorption of large amounts of latent heat. The latent heat absorption causes enhancement of the cooling performance. In this regard, the next-generation cooling technology using flow boiling heat transfer has been actively suggested and researched to enhance thermal management systems, such as nuclear power plants and thermal-hydraulic systems. Many studies have been conducted to enhance the boiling heat transfer (e.g., heat transfer coefficient and critical heat flux). The heat transfer coefficient (HTC) represents heat transfer efficiency, while the critical heat flux (CHF) means the maximum limitation of heat flux range, simultaneously representing the boiling performance. CHF is a crucial factor determining the operating limit of boiling heat transfer applications. When CHF occurs, the nucleation accelerates, forming the vapor film on the surface. The vapor film acts as the insulation layer due to its low thermal conductivity, blocking the heat transfer and increasing the surface temperature (i.e., temperature peak). Therefore, the CHF enhancement was needed to improve the boiling heat transfer performance. In this regard, research on CHF enhancement have been actively conducted by using micro/nano-structures due to their high liquid-supply capacity (i.e., wicking and re-wetting flow). A high liquid-supply capacity during the boiling can delay the vapor film formation even at high heat flux conditions, resulting in CHF enhancement.

Meanwhile, the bubble behavior during the flow boiling process changes along the flow direction (i.e., nucleation → bubble merging → vapor film formation), resulting in the non-uniform thermal distribution on the heated surface. Based on this fact, the local thermal analysis during the flow boiling process needs to be performed to investigate the boiling performance in detail. In this study, we introduced the optical fiber temperature measurement to analyze the high-spatial and temporal thermal distribution during the flow boiling process. Then, we evaluated the boiling performance enhancement using the micro-pillar structure (MPS), which had a high liquid supply capacity in the previous literature [4, 5], by measuring the surface temperature distribution using the optical fiber sensor.

2. Research methods and results

2.1. MPS sample fabrication

We fabricated the MPS sample using the micro-electro-mechanical systems (MEMS) process. MEMS processes for MPS sample fabrication were conducted as follows: cleaning a Si wafer; spin coating using positive PR; photolithography; DRIE process; and asher process. We previously evaluated the liquid supply capacity during the boiling process by measuring the wicking and re-wetting flow performance with various geometries (e.g., pillar diameters and gaps)[4, 5]. The present study used a MPS sample with a diameter of 20 um and a gap of 20 um, which showed a large re-wetting performance in the previous tests. The pillar's height was 15 um. Figures 1(a) and (b) show the schematic and SEM images of the MPS sample used in the present study.

2.2 Flow boiling test loops

Figure 2 shows the experimental schematic of the flow boiling test loops. We used a rectangular single-side heating channel flow loop to perform flow boiling heat transfer tests. The channel has a width of 8 mm and a height of 8 mm. The flow boiling test loop consists of two loops. The main-test loop conducted the local thermal analysis (i.e., surface temperature distribution measurement) and visualized the bubble behaviors. The secondary loop supplied heat to the working fluid (i.e., DI water). All loops have chillers to maintain the fluid temperature (main loop: VB-7, -20 °C ~ 100 °C and secondary loop: RW-0525G, -25 °C ~ 150 °C). A plate-type heat exchanger (70,000 kcal/h) was used for heat exchange between the main and the secondary loops. The inlet temperature was controlled from 70 to 90 ℃ (i.e., sub-cooling temperature was 30 to 10 ℃). Reynolds number (i.e., flow rate) in a flow channel was controlled in the range of 6000 to 10000 using the magnetic gear pump (WT3000-1JB). Then, the flow rate was measured by the gear flow meter (OM008S) and monitored by the panel flow indicator. The flow channel's inlet and outlet temperature was measured using k-type thermocouples (SCAXL-062U-3).

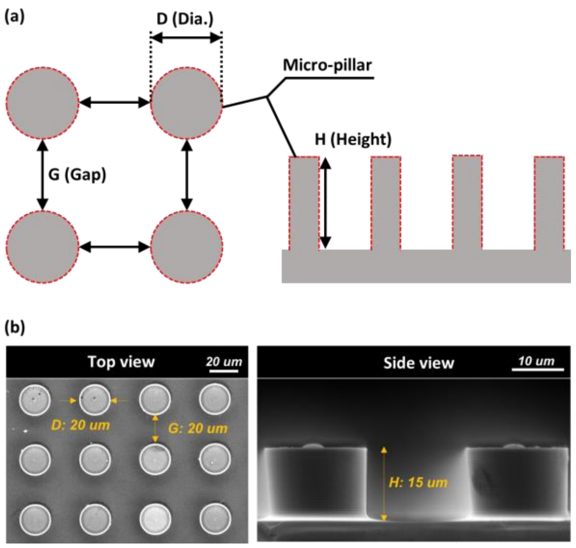

Figure 1 Schematic (a) and SEM images (b) of the MPS sample used in the present study

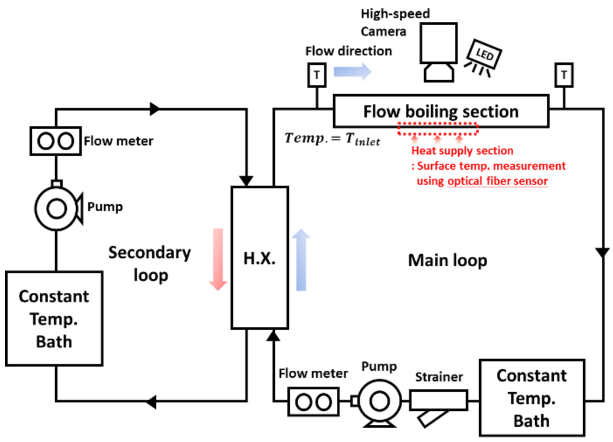

Figure 2 Experimental schematic of the flow boiling test

2.3 Surface temperature measurement using an optical fiber temperature sensor

In this study, the optical distributed sensor interrogator (LUNA, ODiSI 7100 series) was used to measure the surface temperature distribution with high resolution. The LUNA ODiSI equipment uses the optical frequency domain reflectometry (OFDR) to obtain the Rayleigh backscattered signal throughout the optical fiber. The fiber expansion owing to temperature changes causes a refraction of the backscattered signal, resulting in a signal's frequency shift. Based on this fact, we can calculate the temperature change (ΔT) using this frequency shift (f_{shift}) throughout the optical fiber as follows.

$$\Delta T = T - T_{ref} = f(f_{shift}) \qquad (1)$$

The frequency shift function (equation 1) was found to be highly accurate (within an error of 2%) when compared with the measured temperature of fiber position by the thermocouple sets in the repeatability test.

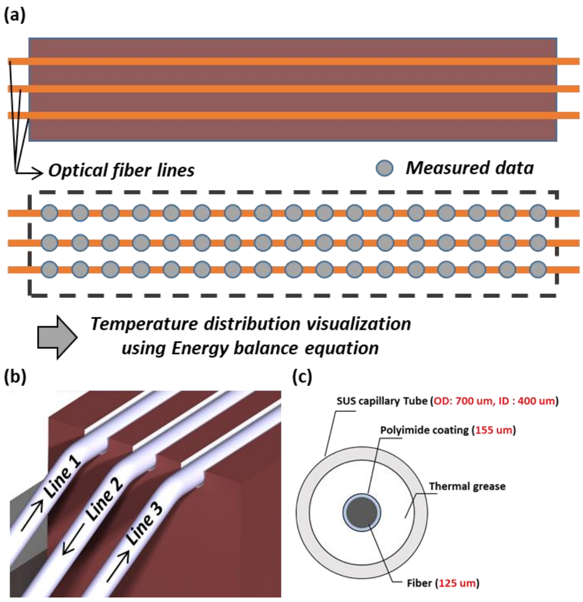

Figure 3 Schematics of optical fiber temperature measurement

Figure 3 shows the schematics of optical fiber temperature measurement in this study. The optical fiber temperature sensor was embedded in the three grooves on the Cu block for a fast response to surface temperature measurements. The optical fiber has a diameter of 155 um including the polyimide coating. The SUS 304 capillary tube (ID: 400 um, OD: 700 um) was used to fix the optical fiber temperature sensor, maintaining the free-strain state. The thermal grease (thermal conductivity of 12.5W/m·K, -250 ~ 350 ℃) was filled in the SUS capillary tube to reduce thermal contact resistance. The thermal grease's high-temperature limit (~350 ℃) can ensure that the grease has a liquid property even at high temperatures. For this reason, the fiber embedded in the thermal grease was not affected by the grease's thermal expansion in the boiling test range, maintaining the free-strain state. The data interpolation at the non-measurement points was conducted using the energy balance equation to visualize the surface temperature distribution. The temperature calculation and 3-D mapping were performed by using the Matlab code.

2.4 Surface temperature measurement results

Figures 4(a) and (b) show the surface temperature distribution on the plain surface and the MPS sample near the CHF, respectively. The inlet temperature was 80 ℃ with Reynolds number of 6000. The supplied heat flux was about 130 W/cm^2. For the flow boiling tests, the plain surface had a CHF of about 133 W/cm^2, while the MPS sample showed a CHF of about 140 W/cm^2. As shown in Figure 4, the MPS sample had a significantly reduced temperature distribution compared to the plain surface. Especially, the center region of the MPS sample showed a significantly reduced temperature distribution. This finding implies that the center region was affected by the continuous re-wetting flow induced by wicking.

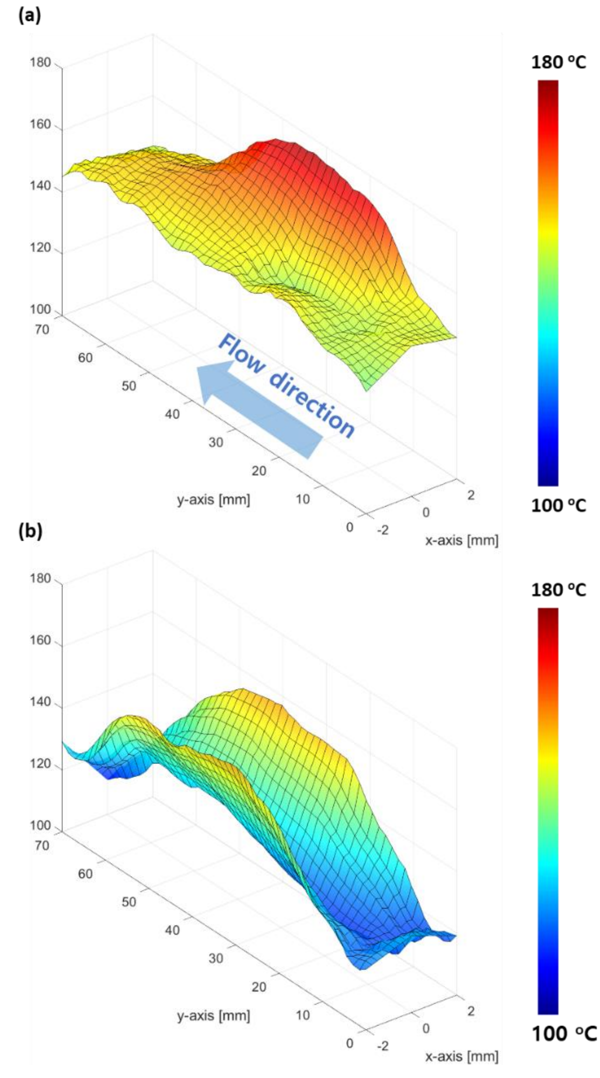

Figure 4 Surface temperature distribution on the plain surface (a) and the MPS sample (b) at the inlet temperature of 80 ℃ and the Reynolds number of 6000

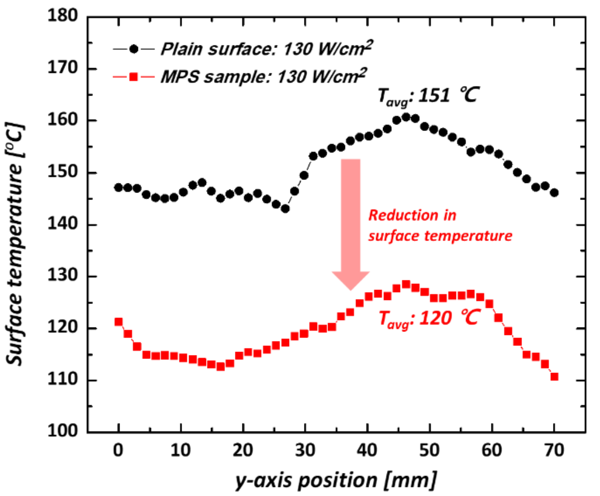

Figure 5 Surface temperature comparison between the plain surface and the MPS sample at the heat flux of 130 W/cm^2

Figure 5 compares the centerline temperature profile between the plain surface and the MPS sample at the heat flux of 130 W/cm^2. As shown in Figure 5, the MPS sample showed a significant reduction of surface temperature. The averaged surface temperature on the MPS sample was 120 ℃, 21% lower than that on the plain surface (~ 151 ℃). The re-wetting flow into the bubble base on the MPS sample can continuously quench the heated surface, decreasing the surface temperature.

3. Conclusions

This study used an optical fiber temperature sensor to conduct local thermal analysis during the flow boiling process. Visualizing the surface temperature distribution confirmed that the MPS sample, which had a high liquid supply capacity (i.e., large re-wetting flow), showed a significantly reduced surface temperature. Based on this finding, we confirmed that the large re-wetting flow performance contributed to CHF enhancement and surface temperature reduction owing to continuous quenching of the heated surface. Additionally, the bubble behavior can be associated with the surface temperature profile (i.e., pattern). In the surface temperature profile shown in Figure 5, the surface temperature rose at the rear end (i.e., 35 mm ~) on both test samples, resulting from local bubble merging and vapor film formation at the rear end in the flow channel. These findings imply that measuring the surface temperature distribution using optical fiber can contribute to the local thermal analysis of non-uniform thermal systems such as the flow boiling heat transfer system. Conclusively, the measurement methodology using the optical fiber temperature sensor for local thermal analysis and the CHF evaluation introduced in this study are expected to provide helpful guidelines for further studies about the local thermal analysis in various thermal management systems.

Acknowledgement

This work was partly supported by the Basic Science Research Program through the NRF funded by the Ministry of Education (Grant Number: NRF-2021R1I1A3052326) and by KEPCO Nuclear Fuel funded by the Korea government (Ministry of Trade, Industry and Energy).

REFERENCES

[1] D.E. Kim, D.I. Yu, D.W. Jerng, M.H. Kim, H.S. Ahn, Review of boiling heat transfer enhancement on micro/nanostructured surfaces, Exp Therm Fluid Sci, 66 (2015) 173-196.

[2] Y. Song, S. Gong, G. Vaartstra, E.N. Wang, Microtube Surfaces for the Simultaneous Enhancement of Efficiency and Critical Heat Flux during Pool Boiling, ACS Appl Mater Interfaces, 13(10) (2021) 12629-12635.

[3] D.I. Shim, G. Choi, N. Lee, T. Kim, B.S. Kim, H.H. Cho, Enhancement of Pool Boiling Heat Transfer Using Aligned

Silicon Nanowire Arrays, ACS Appl Mater Interfaces, 9(20) (2017) 17595-17602.
[4] H.T. Nam, H.H. Cho, S. Lee, D. Lee, Temperature-dependent wicking dynamics and its effects on critical heat flux on micropillar structures in pool boiling heat transfer, International Communications in Heat and Mass Transfer, 146 (2023) 106887.
[5] H.T. Nam, H.H. Cho, S. Lee, D. Lee, Two-Phase Particle Image Velocimetry Visualization of Rewetting Flow on the Micropillar Interfacial Surface, ACS Applied Materials & Interfaces, 16(26) (2024) 34313-34325.